Neuroscience and Biobehavioral Reviews 183 (2026) 106554

Contents lists available at ScienceDirect

Neuroscience and Biobehavioral Reviews

journal homepage: www.elsevier.com/locate/neubiorev

Gray matter atrophy and structural connectivity in Posterior Cortical Atrophy: A voxel-based meta-analysis

Daniele Licciardo [a,c,*], Chiara Matti [d], Alberto Benelli [e], Valeria Isella [a,b], Ildebrando Appollonio [a,b], Emiliano Santarnecchi [c]

[a] School of Medicine and Surgery, University of Milano-Bicocca, Monza, Italy
[b] Neurology Department, Fondazione IRCCS San Gerardo dei Tintori, Monza, Italy
[c] Precision Neuromodulation Program & Network Control Laboratory, Gordon Center for Medical Imaging, Department of Radiology, Massachusetts General Hospital, Harvard Medical School, Boston, MA, USA
[d] Neuro X Institute, Swiss Federal Institute of Technology Lausanne (EPFL), Lausanne, Switzerland
[e] Siena Brain Investigation and Neuromodulation Lab, Department of Medicine, Surgery and Neuroscience, University of Siena, Siena, Italy

ARTICLE INFO

Keywords:
Posterior Cortical Atrophy
Alzheimer's disease
Neuroimaging
Coordinate-based approach
Meta-analysis
VBM
SDM

ABSTRACT

Posterior Cortical Atrophy (PCA) is a neurodegenerative syndrome most commonly associated with Alzheimer's disease, characterized by progressive visuospatial and visuoperceptual decline. Although voxel-based morphometry studies have described gray matter loss in PCA, a comprehensive and updated coordinate-based meta-analysis is still missing, and associated structural connectivity alterations remain unclear. We conducted a systematic review and meta-analysis of whole-brain voxel-based morphometry studies comparing patients with PCA and healthy controls (PROSPERO ID: CRD420251010673). Analyses were performed using Seed-based d Mapping with Permutation of Subject Images (SDM-PSI) with family-wise error correction, and meta-regressions assessed the impact of demographic and clinical variables. To investigate structural connectivity, deterministic tractography was carried out on a normative diffusion MRI template, using meta-analytic gray matter clusters as seeds. Eighteen studies were included (339 PCA; 577 healthy controls). The meta-analysis revealed consistent bilateral gray matter atrophy in the lateral occipital cortex, inferior parietal lobule, precuneus, and ventral occipitotemporal regions. Meta-regression highlighted an interaction between age and disease duration, associated with atrophy in the left superior temporal gyrus and right thalamus. Tractography demonstrated that affected clusters were embedded within major long-range pathways, including the superior and inferior longitudinal fasciculi, vertical occipital fasciculi, and parietal aslant tract. Regression-derived clusters additionally mapped onto the arcuate fasciculus, frontal aslant tract, and superior thalamic radiations. This is the first systematic review and voxel-based meta-analysis of PCA conducted after the establishment of consensus diagnostic criteria, providing a statistically robust characterization of gray and white matter alterations and identifying potential imaging biomarkers for diagnosis and treatment.

1. Introduction

Posterior Cortical Atrophy (PCA) is a complex clinical-radiological syndrome characterized by progressive neurodegeneration predominantly affecting the parietal, occipital, and occipitotemporal cortices (Benson et al., 1988; Crutch et al., 2012). Clinically, PCA is marked by a progressive decline in higher-order visual processing, with relative preservation of memory and language in the early stages. It is most commonly associated with Alzheimer's disease (AD) pathology and is widely recognized as the "posterior" or "visuospatial" variant of the disease (Chapleau et al., 2024; Dubois et al., 2014; McKhann et al., 2011). Although PCA accounts for only ~5 % of cases seen in memory clinics (Koedam et al., 2010; Snowden et al., 2007), its impact is significant due to its typically presenile onset and consequent implications for quality of life and functional independence (Ahmed et al., 2020; Schott and Crutch, 2019; Tang-Wai et al., 2004).

While PCA can often be detected on visual inspection of structural MRI, advanced neuroimaging techniques have been developed to

* Correspondence to: School of Medicine and Surgery, University of Milano-Bicocca, Via Cadore 48, Monza 20900, Italy.
E-mail addresses: d.licciardo@campus.unimib.it (D. Licciardo), chiara.matti@epfl.ch (C. Matti), albertobenelli21@gmail.com (A. Benelli), valeria.isella@unimib.it (V. Isella), ildebrando.appollonio@unimib.it (I. Appollonio), esantarnecchi@mgh.harvard.edu (E. Santarnecchi).

https://doi.org/10.1016/j.neubiorev.2026.106554
Received 5 September 2025; Received in revised form 17 December 2025; Accepted 11 January 2026
Available online 28 January 2026

quantify and localize gray matter (GM) loss more precisely. Among these, voxel-based morphometry (VBM) is one of the most widely used methods for investigating whole-brain atrophy in neurodegenerative conditions (Crane et al., 2024; Velioglu et al., 2023), offering automated, operator-independent, and hypothesis-free group comparisons.

To date, only one coordinate-based meta-analysis (CBMA) has systematically investigated GM atrophy in PCA using VBM data (Alves et al., 2013). In that study, Alves et al. (2013) applied Effect Size Signed Differential Mapping (ES-SDM) to synthesize VBM findings, identifying significant GM volume reductions in PCA patients compared to healthy controls (HCs), predominantly in the left temporal and occipital cortices (including the inferior and middle temporal gyri, fusiform, parahippocampal, and middle occipital gyrus), as well as in right temporo-parietal regions (middle and superior temporal gyri, and inferior parietal lobule). However, the study had key methodological limitations: it included only four studies (one of which was a single case report), totaling 104 PCA patients and 76 HCs; used outdated meta-analytic software that lacked family-wise error (FWE) correction; and was conducted prior to the publication of internationally recognized diagnostic criteria for PCA (Crutch et al., 2017). Furthermore, since 2013 numerous VBM studies have emerged, providing a richer and more robust evidence base to reassess the neuroanatomical profile of PCA. These developments underscore the need for an updated and methodologically robust meta-analysis.

Beyond cortical atrophy, growing evidence from whole-brain diffusion tensor imaging (DTI) studies suggests that PCA is also associated with widespread white matter (WM) degeneration (Cerami et al., 2015; Madhavan et al., 2016; Migliaccio et al., 2012a; Millington et al., 2017; Phillips et al., 2024). Reported abnormalities are heterogeneous, affecting the inferior longitudinal fasciculus (ILF), superior longitudinal fasciculus (SLF), inferior fronto-occipital fasciculus (IFOF), cingulum, uncinate fasciculus, posterior thalamic radiations, corpus callosum segments, and both parietal and frontal aslant tracts (PAT, FAT). These alterations have been described as following a bilateral posterior-to-anterior gradient (Migliaccio et al., 2012a; Phillips et al., 2024), though some studies suggest greater right-hemisphere involvement (Cerami et al., 2015; Madhavan et al., 2016). Nonetheless, this literature remains limited, as most studies rely on region-specific approaches and small PCA samples (typically fewer than 20 patients).

To address these gaps, the present study aimed to (i) provide an updated and statistically rigorous meta-analysis of VBM findings in PCA using Seed-based d Mapping with Permutation of Subject Images (SDM-PSI), a next-generation CBMA technique that incorporates multiple imputation of study images and threshold-free cluster enhancement (TFCE) for improved sensitivity and control of false positives (Albajes-Eizagirre et al., 2019c; Liberati et al., 2009; Müller et al., 2017); and (ii) explore the structural connectivity of the resulting meta-analytic GM atrophy maps using deterministic tractography based on a population-averaged diffusion MRI template. This integrative approach offers a comprehensive framework for characterizing both GM and WM alterations in PCA and lays the foundation for future studies aimed at improving early diagnosis, understanding disease progression, and identifying network-level therapeutic targets.

2. Methods

2.1. Study design and registration

The present meta-analysis was conducted in accordance with the Preferred Reporting Items for Systematic Reviews and Meta-analyses (PRISMA) statement (Liberati et al., 2009) (the corresponding checklist is provided in the Supplementary Material S1), following the guidelines and recommendations for CBMA (Müller et al., 2017), and has been pre-registered in PROSPERO (registration number: CRD420251010673, https://www.crd.york.ac.uk/prospero/). Based on the meta-analytic results, a structural connectivity study was subsequently performed through a normative-connectivity approach. The pipeline of the study is provided in Fig. 1.

2.2. Study selection and eligibility criteria

A comprehensive and systematic literature search was conducted from inception to April 2025 across five electronic databases: PubMed, Scopus, Web of Science, Embase, and MEDLINE. To ensure thorough identification of relevant studies, we also screened the supplementary materials of eligible articles and reference lists of relevant reviews for additional studies. The search strategy combined free-text keywords and MeSH terms using Boolean operators (AND, OR) to maximize sensitivity and specificity. The strategy was initially piloted to refine descriptors and subsequently harmonized across databases using the Polyglot Search Translator (Clark et al., 2020). The final search string was: ("Posterior Cortical Atrophy") OR ("visual variant" AND Alzheimer) AND ("Magnetic Resonance Imaging" OR MRI OR "Neuroimaging" OR "Brain Mapping" OR voxel* OR VBM). Database-specific search strategies are provided in the Supplementary Material (S2 - Search terms by database).

The results from each database were imported into Covidence (https://www.covidence.org/), a platform designed to facilitate the management and execution of the multiple stages of a systematic review by automatically removing duplicates and assisting with data screening and extraction.

Eligible studies had to meet the following inclusion criteria: (1) VBM studies that performed whole-brain GM analysis and reported brain coordinates in MNI or Talairach space; (2) studies including patients with PCA-pure, diagnosed based on or following consensus criteria (Crutch et al., 2017), and HCs for comparison.

Studies were excluded if they met any of the following exclusion criteria: (1) non-peer-reviewed publications (e.g., preprints and conference abstracts) or review articles; (2) studies including patients with PCA-plus (Crutch et al., 2017), characterized by additional features of other neurodegenerative syndromes such as Dementia with Lewy Bodies (DLB), Corticobasal Syndrome (CBS), or Primary Progressive Aphasia (PPA); (3) single-case studies.

Two independent reviewers screened titles, abstracts, and full texts according to predefined inclusion and exclusion criteria. Clinical classification (e.g., PCA pure and PCA plus) was independently verified by two neurologists, and any discrepancies, whether arising during the screening phase or diagnostic classification, were resolved by consensus or, if necessary, by a third reviewer.

At the end of the selection process, 18 studies comprising 19 independent samples were included in the meta-analysis (Fig. 2).

2.3. Data extraction and quality assessment

A standardized electronic data extraction form was developed in Covidence to systematically collect relevant study information, including study design, sample size, demographic and clinical characteristics of participants, diagnostic criteria for PCA, and imaging parameters.

The primary outcomes of interest were GM volume reductions in PCA compared with HCs, reported as three-dimensional peak coordinates in either MNI or Talairach space, together with the corresponding statistical values and thresholds.

Brain coordinates extracted from studies were cross-checked using the Automated Anatomical Labeling (AAL) atlas in SPM (https://www.fil.ion.ucl.ac.uk/spm/). In cases of unclear data, study investigators were contacted via email for clarification.

For quality assessment, two independent reviewers evaluated the methodological quality and risk of bias of each included study using the Newcastle-Ottawa Scale (NOS) (Wells et al., 2014), a widely used tool for evaluating the quality of observational studies. The 9-point NOS checklist applied in this study is provided in the Supplementary Material S3.

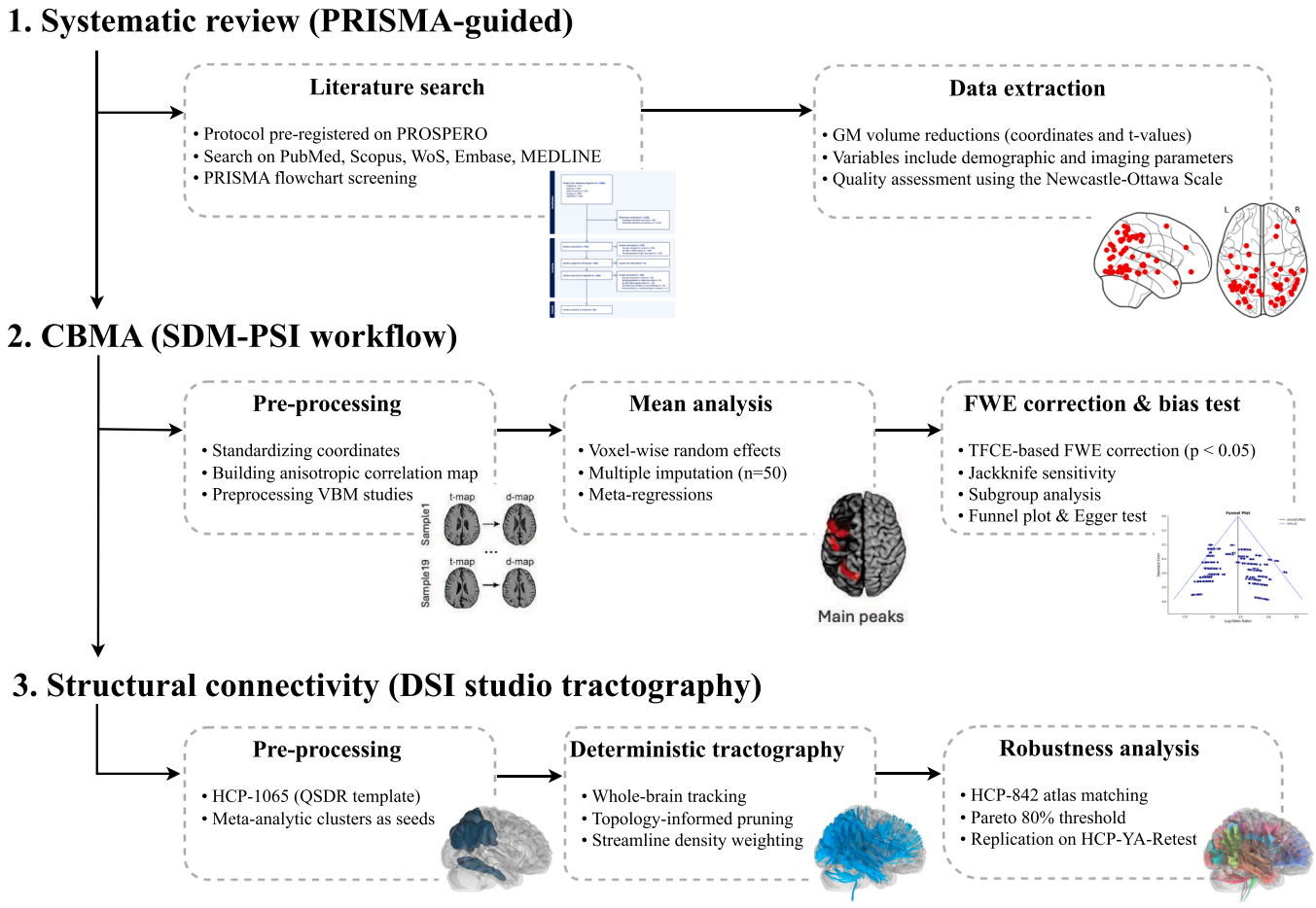

Fig. 1. Overview of the methodological pipeline. The figure illustrates the three main stages of the study: (1) Systematic review (PRISMA-guided): The protocol was pre-registered on PROSPERO, and the literature search was conducted across PubMed, Scopus, Web of Science, Embase, and MEDLINE. Records were screened according to PRISMA guidelines, and data extraction included demographic and clinical variables, stereotactic coordinates, and effect sizes. Study quality was assessed using the Newcastle–Ottawa Scale. (2) Coordinate-based meta-analysis (CBMA) using Seed-based d Mapping with Permutation of Subject Images (SDM-PSI): Reported coordinates were standardized within a voxel-based morphometry (VBM) gray-matter correlation template and used to build anisotropic correlation maps. Mean and regression analyses were performed using voxel-wise random-effects modeling with multiple imputations ($n = 50$), applying Threshold-Free Cluster Enhancement (TFCE)-based Family-Wise Error (FWE) correction ($p < 0.05$) and assessing jackknife sensitivity, subgroup effects, and publication bias. (3) Structural connectivity (DSI Studio tractography): Deterministic tractography was applied to the population-averaged HCP-1065 diffusion MRI template reconstructed through Q-space Diffeomorphic Reconstruction (QSDR). Meta-analytic gray matter clusters served as seed regions for whole-brain fiber tracking, with tracts classified via the HCP-842 atlas and robustness confirmed through Pareto-based thresholding and replication on the HCP-YA-Retest dataset.

2.4. CBMA and meta-regression

CBMA was performed using SDM-PSI software package (version 6.23 for Mac, https://www.sdmproject.com/) following a structured approach (Radua and Mataix-Cols, 2009). First, peak coordinates and their corresponding t-values of significant GM differences between PCA patients and HCs were extracted. Then, maps of the lower and upper bounds of possible effect sizes were computed within a GM mask, using full anisotropy = 1, an isotropic full-width half maximum (FWHM) of 20 mm, and a voxel size of 2 mm. The mean analysis was conducted by estimating the most likely effect size and its standard error based on the MetaNSUE algorithms (Albajes-Eizagirre et al., 2019b). Multiple imputations of the effect size maps for individual studies were then performed, followed by a meta-analysis using a standard random-effects model and Rubin's rules to pool the results of the multiple imputations. To correct for multiple comparisons, FWE correction was applied, and statistical thresholding was refined using TFCE with a significance threshold of $p < 0.05$ and a voxel extent ≥ 50, which was selected to balance sensitivity and specificity (Radua et al., 2012; Smith and Nichols, 2009; Yang et al., 2023). Further methodological details can be found in previous publications (Albajes-Eizagirre et al., 2019a, 2019c), and in the SDM-PSI reference manual (https://www.sdmproject.com/manual/).

Finally, meta-regression analyses were conducted to examine the potential influence of demographic and clinical variables including age, gender, education, disease duration (time from symptom onset to MRI acquisition) and MMSE score on GM. These analyses were performed using linear regression, with predictors weighted by the square root of the sample size, as implemented in the SDM method (Radua et al., 2014). A stringent threshold of $p < 0.05$ and cluster extent ≥ 50 voxels was applied to ensure robust results (Higgins et al., 2003; Radua and Mataix-Cols, 2009; Smith and Nichols, 2009).

2.5. Robustness, heterogeneity and publication bias

To assess the robustness of the findings, a whole-brain voxel-based jackknife sensitivity analysis was conducted using a leave-one-out approach (Albajes-Eizagirre et al., 2019c; Radua and Mataix-Cols, 2009). This procedure systematically re-ran the meta-analysis, omitting one study at a time, to verify whether the main results remained stable across all possible study combinations.

To explore the potential influence of methodological variability,

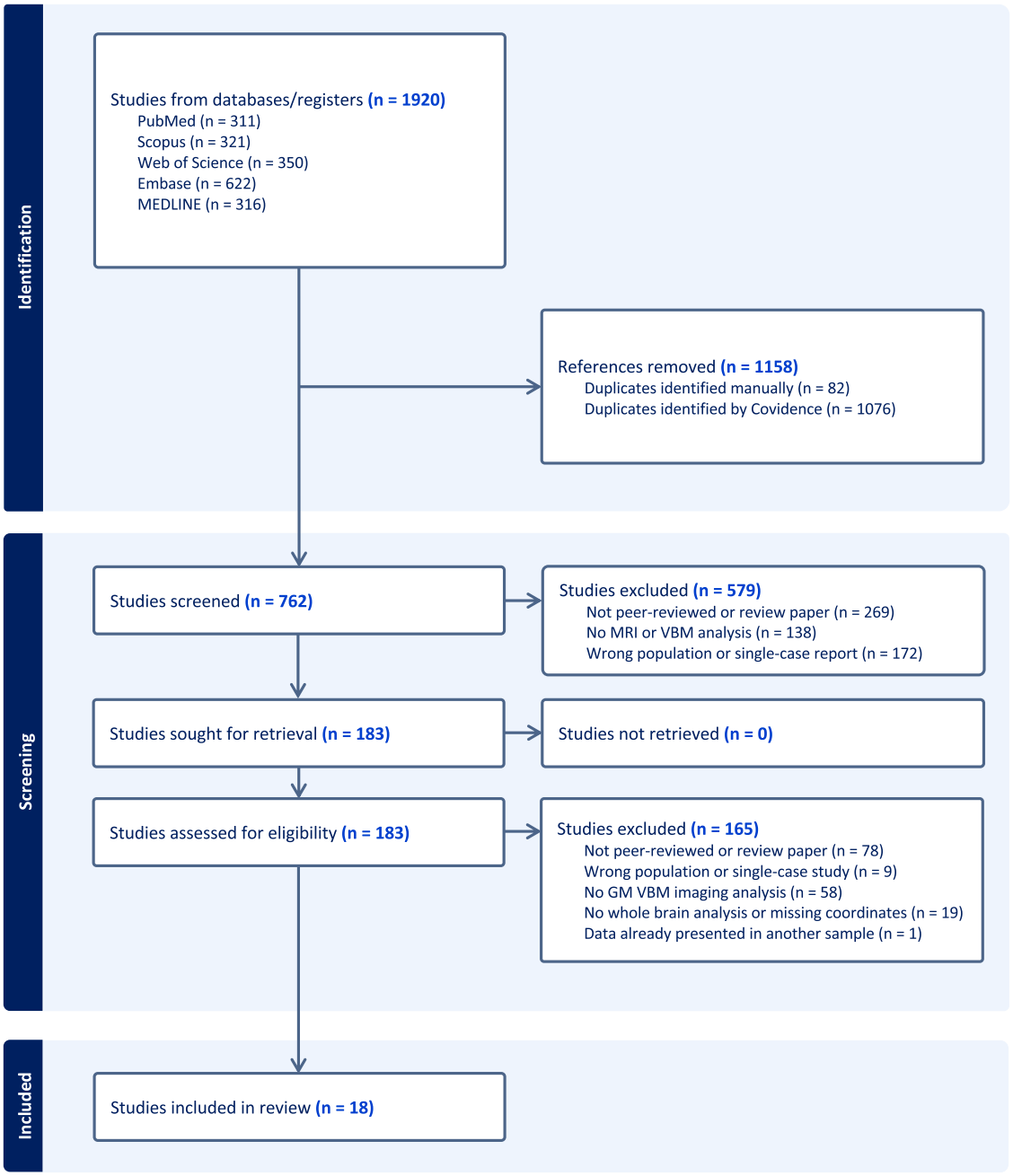

Fig. 2. Flow diagram of study selection for VBM articles in PCA (via Covidence). Acronyms: VBM = Voxel-Based Morphometry; GM = Gray Matter.

subgroup meta-analysis were performed based on key imaging parameters. Specifically, subgroups were defined according to the use of a 3.0 T MRI scanner, SPM version 12, a smoothing kernel $\geq$ 8 mm, and the application of corrected statistical thresholds. Each subgroup analysis was conducted using a TFCE-based FWE-corrected threshold ($p < 0.05$, voxel extent ≥ 50). A replication index was quantified by calculating the proportion of significant voxels from the main meta-analysis that were also present in each subgroup analysis, using the formula:

$$R = \frac{|A \cap B|}{|A|}$$

where A is the set of significant voxels in the main analysis, and B is the corresponding set in the subgroup analysis.

Heterogeneity was examined using the I^2 statistic at each peak coordinate identified in the CBMA to assess between-study variability at key regions, with $I^2 < 50$ % interpreted as low heterogeneity (Egger et al., 1997). Publication bias was evaluated through visual inspection of funnel plots and by performing Egger's test (Eickhoff et al., 2011). Evidence of funnel plot asymmetry or a p-value < 0.05 in the Egger's test was considered indicative of potential publication bias.

The overall certainty of the cumulative evidence was qualitatively evaluated based on jackknife stability, replication across subgroup analyses, and between-study heterogeneity (I^2).

2.6. Structural connectivity analysis

To examine potential microstructural connectivity alterations in PCA, we employed a normative-connectivity (indirect mapping) approach (Dogan et al., 2015; Jiang et al., 2023; Li et al., 2021; Liang et al., 2023; Phillips et al., 2019; Ravano et al., 2021; Salvalaggio et al., 2020; Smits et al., 2023). Accordingly, statistically significant

meta-analytic atrophy clusters were treated as a single, spatially distributed region of interest and projected onto a population-averaged structural connectome derived from 1065 healthy adults (575 females; aged 22–37 years) from the HCP-1065 dataset (Yeh, 2022) (https://db.humanconnectome.org), allowing standardized inference on the WM pathways most likely associated with the observed atrophy pattern without relying on patient-level diffusion data (Phillips et al., 2019).

Tractography was performed in DSI Studio (https://dsi-studio.labsolver.org) in two separate analyses. First, a composite seed mask comprising all significant clusters from the main CBMA map was used to estimate the principal disconnection pattern associated with convergent GM atrophy. Second, an independent composite seed mask including all significant clusters from meta-regression map was used to explore moderator-related disconnection patters.

Diffusion data for the HCP-1065 template were acquired with a multishell scheme (b = 1000–3000 s/mm^2; 90 directions; 1.25 mm isotropic) and reconstructed in MNI space using q-space diffeomorphic reconstruction to obtain the spin distribution function (Yeh et al., 2010; Yeh and Tseng, 2011).

Tracking parameters were randomly sampled from predefined ranges to enhance robustness and reproducibility (Otsu, 1979; Yeh, 2020): the anisotropy threshold ranged from 0.5 to 0.7 times the Otsu threshold, the angular threshold from 15° to 90°, and step size from 0.5 to 1.5 voxel lengths. A maximum of one million seeds was used for the fiber tracking. To improve anatomical accuracy, each streamline was matched with the closest trajectory in the HCP842 atlas (http://brain.labsolver.org) using the shortest Hausdorff distance (Yeh et al., 2018), and further refined through 20 iterations of topology-informed pruning (Yeh et al., 2019). A Pareto-based criterion was then applied to retain tracts cumulatively accounting for 80 % of total streamline contributions, capturing the dominant structural pathways while reducing redundancy and noise (Miettinen, 2003; Siless et al., 2017; Yeh et al., 2018).

Robustness analyses were conducted at two complementary levels. First, tractography analyses were replicated on an independent population-averaged diffusion template (HCP-YA Retest; N = 88; ages 22–35) (Glasser et al., 2013; Van Essen et al., 2013) (https://github.com/data-hcp/lifespan/releases), processed using the same pipeline as the HCP-1065 template. Agreement across templates was quantified using a replication index (defined as the proportion of reproduced WM pathways) and Spearman rank correlations of tract-wise contributions. Second, robustness with respect to the tractography seeding strategy was assessed via cluster-wise sensitivity analyses, in which tractography was repeated using each significant cluster as an independent seed, separately for the main CBMA and the meta-regression analyses. Similarity between composite- and cluster-derived pathway sets was quantified using the Jaccard index (Grady et al., 2021).

3. Results

3.1. Included studies and sample characteristics

Eighteen studies with 19 samples were included, comprising 916 participants (339 PCA and 577 HCs) (Agosta et al., 2018; Ahmed et al., 2018; Cope et al., 2022; Cui et al., 2022; Fredericks et al., 2019; Fumagalli et al., 2020; Glick-Shames et al., 2019; Lehmann et al., 2011; Migliaccio et al., 2016, 2012b, 2009; Miller et al., 2018; Montembeault et al., 2018; Neitzel et al., 2016; Ramanan et al., 2018; Ranasinghe et al., 2014; Ryan et al., 2014; Whitwell et al., 2007).

Across studies, the mean age of PCA participants ranged from 57.6 to 68.8 years, with women representing 57 % of the group (n = 195), whereas healthy controls had mean ages ranging from 54.9 to 69.5 years and included 54 % women (n = 315). No significant differences were found between the PCA and HC groups in terms of age (standardized mean difference [SMD] = −0.08, 95 % confidence interval [CI] = [−0.30, 0.14], z = −0.70, p = 0.48), education (reported in 10 studies; SMD = 0.02, 95 % CI = [−0.90, 0.93], z = 0.04, p = 0.97), or gender ratio (SMD = 0.07, 95 % CI = [−0.03, 0.16], z = 1.37, p = 0.17).

The mean NOS quality score across the VBM studies was 7.61 out of 9 (range 6–9; see individual NOS ratings in Supplementary Material S4) indicating that the included studies were of high quality. Demographic, clinical, and quality characteristics of each eligible study are summarized in Table 1, while Supplementary Material S5 provides detailed technical parameters and the number of significant peaks reported in each study.

3.2. CBMA and meta-regression

The CBMA revealed three clusters of significant GM reduction in PCA patients compared to HCs (Fig. 3 and Table 2). The largest cluster (5593 voxels, SDM-Z = 4.71, p < 0.001) was centered in the right middle occipital gyrus and extended to the right inferior parietal lobule, angular gyrus, and ventral occipito-temporal regions. A second cluster (3612 voxels, SDM-Z = 4.74, p < 0.001) was located in the left superior occipital gyrus, involving the bilateral precuneus and left occipital regions. The third cluster (937 voxels, SDM-Z = 4.64, p < 0.001) was centered in the right inferior temporal gyrus, extending into the middle temporal cortex.

Meta-regression analyses revealed no significant associations with gender, education level, or MMSE scores. Given the strong and significant negative correlation between mean age and disease duration across samples (r = −0.78, p < .001; i.e., samples with younger participants had longer disease duration), separate meta-regressions for these two variables were considered potentially confounded and difficult to interpret. Therefore, a multiple meta-regression was performed including both centered variables (age and disease duration) and their interaction term. Only the interaction term (contrast: 0 0 1) yielded significant results (Fig. 4), revealing a cluster in the left superior temporal gyrus (BA 48) (1090 voxels; SDM-Z = 3.19; p < 0.001) and another cluster in the right thalamus (91 voxels; SDM-Z = 3.015; p < 0.01).

3.3. Robustness, heterogeneity and publication bias

The leave-one-out jackknife sensitivity analysis confirmed the robustness of the meta-analysis findings, with all three peaks preserved across all study combinations (Table 2). Subgroup analyses further supported the stability of the results: when the meta-analysis was restricted to studies using a 3.0 T scanner, 95.6 % of the significant voxels from the main map were replicated; 93.7 % were replicated in studies applying FWE-corrected thresholds, 99.5 % in those using SPM12, and 99.9 % in studies employing a smoothing kernel ≥ 8 mm.

There was no substantial heterogeneity among the included studies at the peak coordinates of GM reduction, as indicated by low I^2 values for all three clusters ranging from 5.5 % to 12.2 % (cluster 1 = 5.5 %; cluster 2 = 12.2 %; cluster 3 = 7.6 %).

Funnel plots showed no visible asymmetry (Supplementary Material S6), and Egger's tests were non-significant for all three clusters (cluster 1 bias = 0.90, z = 0.68, p = 0.499; cluster 2 bias = 0.74, z = 0.56, p = 0.578; cluster 3 bias = 1.34, z = 1.06, p = 0.288).

The cumulative evidence showed high certainty, supported by consistent jackknife and subgroup results, low heterogeneity (I^2 < 15 %), and no indication of publication bias.

3.4. Structural connectivity analysis

The tractography analysis based on the meta-analytic GM atrophy map revealed 13 tracts cumulatively accounting for approximately 80 % of the total streamline contribution (Fig. 5, left). The most frequently represented WM pathways were the right PAT (15.6 %), right SLF (III: 9.6 %; II: 6.3 %), and the bilateral vertical occipital fasciculus (VOF; right: 9.3 %, left: 6.5 %). Additional tracts included the ILF (right:

Table 1
Demographic and clinical characteristics of the included VBM studies.

Study	Demographic characteristics								Clinical characteristics		Quality
	Sample size		Age (SD)		Female (%)		Education (SD)		Disease duration (SD)	MMSE (SD)	NOS score
	PCA	HC	PCA	HC	PCA	HC	PCA	HC	PCA	PCA	
Agosta et al. (2018) (S1)	8	24	60.2 (4.7)	60.9 (6.7)	3 (38)	10 (42)	13.6 (2.3)	13 (3.1)	4.8 (1.6)	13.4 (7.4)	7 /9
Agosta et al. (2018) (S2)	13	20	61.9 (6.0)	62.0 (2.8)	9 (69)	13 (65)	9.5 (3.2)	16 (4.7)	3.4 (1.1)	16.5 (4.8)	9 /9
Ahmed et al. (2018)	18	45	64.9 (6.8)	64.4 (7.2)	9 (50)	20 (44)	13.6 (2)	14.2 (3)	3.8 (1.9)	NR (NR)	8 /9
Cope et al. (2022)	15	48	62.5 (8.43)	63.6 (8.2)	9 (60)	26 (54)	NR (NR)	NR (NR)	NR (NR)	19.1 (5.7)	8 /9
Cui et al. (2022)	18	20	57.6 (5.0)	54.9 (8.2)	11 (61)	7 (35)	9.22 (5.2)	11.5 (2.9)	3.94 (1.5)	13.11 (5.3)	9 /9
Fredericks et al. (2019)	26	64	62.1 (7.9)	62.5 (7.6)	14 (54)	34 (53)	16.19 (3.7)	16.42 (1.9)	NR (NR)	22.87 (5.3)	6 /9
Fumagalli et al. (2020)	15	15	68.8 (7.3)	69.5 (6.5)	8 (53)	7 (47)	9.27 (3.8)	7.78 (3.3)	3.6 (2.3)	18.27 (4.7)	9 /9
Glick-Shames et al. (2019)	10	14	63.3 (8.1)	60.9 (7.2)	4 (40)	6 (43)	NR (NR)	NR (NR)	2.88 (NR)	NR (NR)	6 /9
Lehmann et al. (2011)	48	50	63.0 (6.7)	63.7 (9.6)	29 (60)	33 (66)	NR (NR)	NR (NR)	4.8 (NR)	21.4 (4.6)	8 /9
Migliaccio et al. (2009)	14	65	61.0 (8.2)	61.0 (10.1)	9 (64)	38 (58)	15.1 (2.9)	17.6 (2.4)	3.3 (NR)	20.6 (7.2)	8 /9
Migliaccio et al. (2012b)	7	29	60.9 (4.1)	59.0 (4.9)	6 (86)	19 (66)	10.3 (3)	NR (NR)	4 (1.5)	17 (4.9)	7 /9
Migliaccio et al. (2016)	10	28	61.0 (4.0)	57.0 (9.0)	8 (80)	16 (57)	NR (NR)	NR (NR)	3.2 (0.9)	17.5 (5.0)	9 /9
Miller et al. (2018)	19	20	59.2 (6.4)	63.2 (NR)	10 (53)	11 (55)	15.6 (2.1)	NR (NR)	4.2 (6.0)	22.7 (3.8)	7 /9
Montembeault et al. (2018)	27	30	62.6 (5.5)	61.5 (8.4)	15 (56)	16 (53)	NR (NR)	NR (NR)	3.6 (2.3)	19.2 (5.0)	9 /9
Neitzel et al. (2016)	10	12	64.7 (7.5)	64.8 (5.7)	5 (50)	7 (58)	10.2 (1.3)	10.7 (1.8)	2.5 (NR)	19.4 (3.7)	9 /9
Ramanan et al. (2018)	5	10	61.2 (1.5)	66.9 (4.2)	2 (40)	5 (50)	23.8 (2.3)	14 (2.6)	5.5 (2.3)	NR (NR)	7 /9
Ranasinghe et al. (2014)	7	15	60.4 (3.3)	64.1 (5.0)	3 (43)	8 (53)	15.32 (1.9)	16.65 (2.2)	6.64 (2.1)	19.15 (4.6)	6 /9
Ryan et al. (2014)	31	30	63.4 (6.2)	63.9 (6.2)	19 (61)	17 (57)	NR (NR)	NR (NR)	5.3 (2.8)	18.9 (6.4)	7 /9
Whitwell et al. (2007)	38	38	64.3 (7.2)	65.9 (7.0)	22 (58)	22 (58)	14 (NR)	14 (NR)	4 (NR)	18.5 (NR)	6 /9

HCs = Healthy controls; NOS = Newcastle-Ottawa Scale; NR = not reported; PCA = Posterior Cortical Atrophy; S1 = Sample 1; S2 = Sample 2; SD = standard deviations.
Note: S1 and S2 denote two cohorts from the same study, analyzed separately as part of a bi-centric recruitment design.

8.1 %, left: 4.0 %), the forceps major of the corpus callosum (5.8 %), and the right cingulum bundle (4.0 %). Smaller contributions were observed in the left IFOF (3.7 %), corpus callosum body (2.6 %), and left cingulum segments (≤ 2.3 %).

A second tractography analysis, seeded from the atrophy map derived from the meta-regression examining the interaction between centered age and disease duration, identified eight tracts (Fig. 5, right). The largest streamline contributions were found in the left arcuate fasciculus (AF-L: 21.2 %) and the left FAT (13.3 %). Other major pathways included the superior thalamic radiations (STR; right: 11.0 %, left: 5.5 %), left SLF III (7.1 %), the left middle longitudinal fasciculus (MdLF; 9.5 %), left ILF (4.4 %), and the right cingulum (4.3 %).

Robustness analyses showed high agreement across diffusion templates and seeding strategies. Using the HCP-YA Retest template, 81 % of WM pathways identified in the main CBMA analysis and 78 % of those from the age x disease-duration interaction analysis were replicated. Tract-wise contributions showed high consistency across templates ($\rho = 0.87$ and $\rho = 0.84$, respectively; both $p < 0.001$; Supplementary Material S7). Cluster-wise sensitivity analyses further demonstrated near-complete overlap between pathway sets derived from composite and cluster-wise seeding for both statistical maps (main CBMA: Jaccard index = 0.96; age × disease-duration interaction: Jaccard index = 0.87).

4. Discussion

This study provides the most up-to-date and methodologically rigorous CBMA of VBM studies in PCA, complemented by a whole-brain tractography analysis based on a normative diffusion MRI template. By leveraging SDM-PSI and including 18 studies with 19 independent samples (n = 916 participants), we identified a consistent and bilateral pattern of GM atrophy in PCA.

The most significantly affected regions included the right lateral occipital cortex extending into the inferior parietal lobule and ventral occipito-temporal areas, as well as the left superior occipital gyrus and bilateral precuneus. Additional involvement was observed in the right inferior and middle temporal cortices. These findings are aligned with the hallmark clinical and radiological features of PCA (Best et al., 2023).

Compared to the previous meta-analysis by Alves et al. (2013) (), our study both replicates and extends prior findings. Alves and colleagues reported atrophy mainly in the left inferior and middle temporal gyri, fusiform and parahippocampal regions, and the right inferior parietal lobule. In contrast, our results indicate a more pronounced right-lateralized involvement, particularly in occipital and temporal cortices, as well as broader engagement of dorsal and ventral visual streams. Additionally, we consistently identified bilateral precuneus atrophy, a finding not reported by Alves et al., likely reflecting the greater sensitivity of our methodology and the inclusion of a larger, more recent dataset. Notably, this result is consistent with previous studies highlighting the precuneus as a key region for differentiating PCA from DLB (Whitwell et al., 2017), and as a critical area in patients with underlying amyloid pathology (Isella et al., 2022a). Furthermore, the precuneus has been proposed as a promising target for

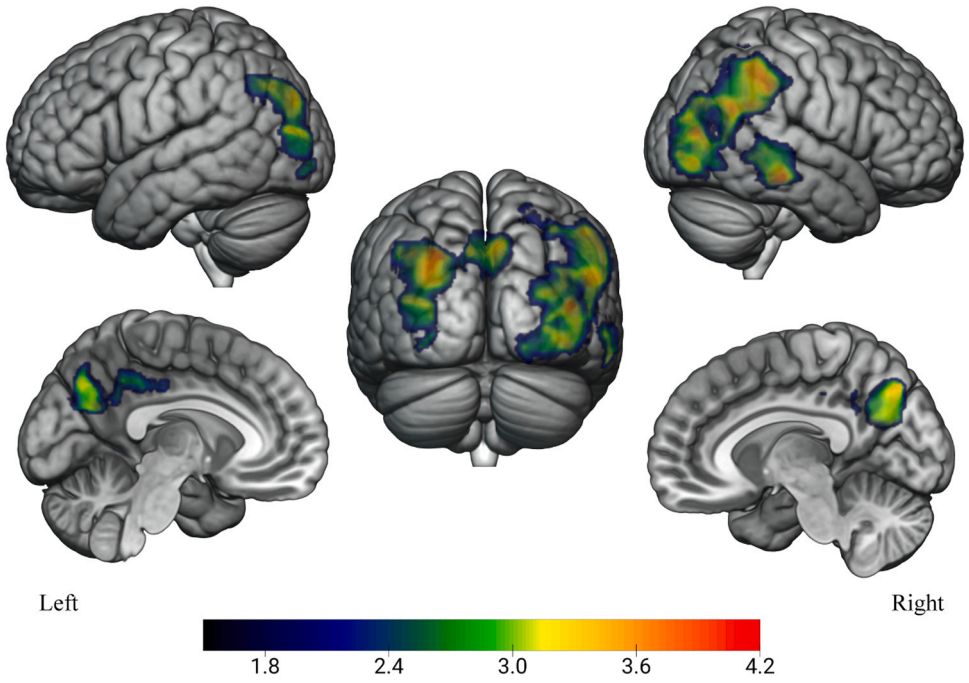

Fig. 3. Regions showing reduced GM in PCA patients. Meta-analytic map of GM volume loss displayed on the MNI152 surface template. FWE correction was applied using TFCE ($p < 0.05$, cluster extent $\geq$ 50 voxels).

Table 2
Regional differences in GM volume between patients with PCA and HCs in the meta-analysis.

Brain regions	MNI coordinates	SDM-Z value	P-value	Number of voxels	Cluster breakdown (number of voxels)	Jackknife sensitivity
Right middle occipital gyrus, BA19	44, −78, 12	4.71	0.0009	5593	Right inferior parietal gyri, BA40 (696); Right middle occipital gyrus, BA19 (519); Right angular gyrus, BA39 (412); Right supramarginal gyrus, BA40 (411); Right inferior occipital gyrus BA19 (299); Right middle temporal gyrus, BA37 (295); Right middle occipital gyrus, BA39 (251); Right fusiform gyrus, BA19 (150)	17 out of 19
Left superior occipital gyrus, BA7	-24, −74, 38	4.74	0.0019	3612	Left middle occipital gyrus, BA19 (757); Corpus callosum (272); Left middle occipital gyrus, BA18 (227); Left precuneus (226); Right precuneus (188); Right precuneus, BA7 (173); Left precuneus, BA7 (166)	18 out of 19
Right inferior temporal gyrus, BA20	60, −30, −16	4.64	0.0019	937	Right middle temporal gyrus, BA21 (456)	19 out of 19

BA = Brodmann area; GM = gray matter; MNI = Montreal Neurological Institute; SDM-Z = Seed-based d Mapping Z-value

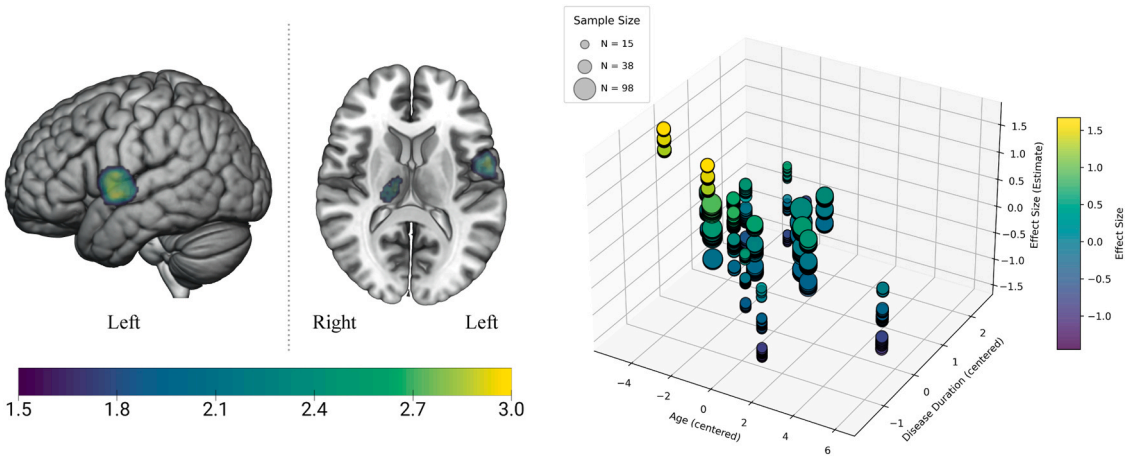

Fig. 4. Brain region showing GM volume associations with age x disease duration interaction in PCA. Meta-regression map and corresponding 3D scatterplot of study-wise effect sizes, visualized as a function of centered age and disease duration. Results are FWE-corrected using TFCE ($p < 0.05$, cluster extent $\geq$ 50 voxels).

neuromodulation interventions in AD (Koch et al., 2022, 2018; Menardi et al., 2021), supporting its relevance in both diagnostic and therapeutic

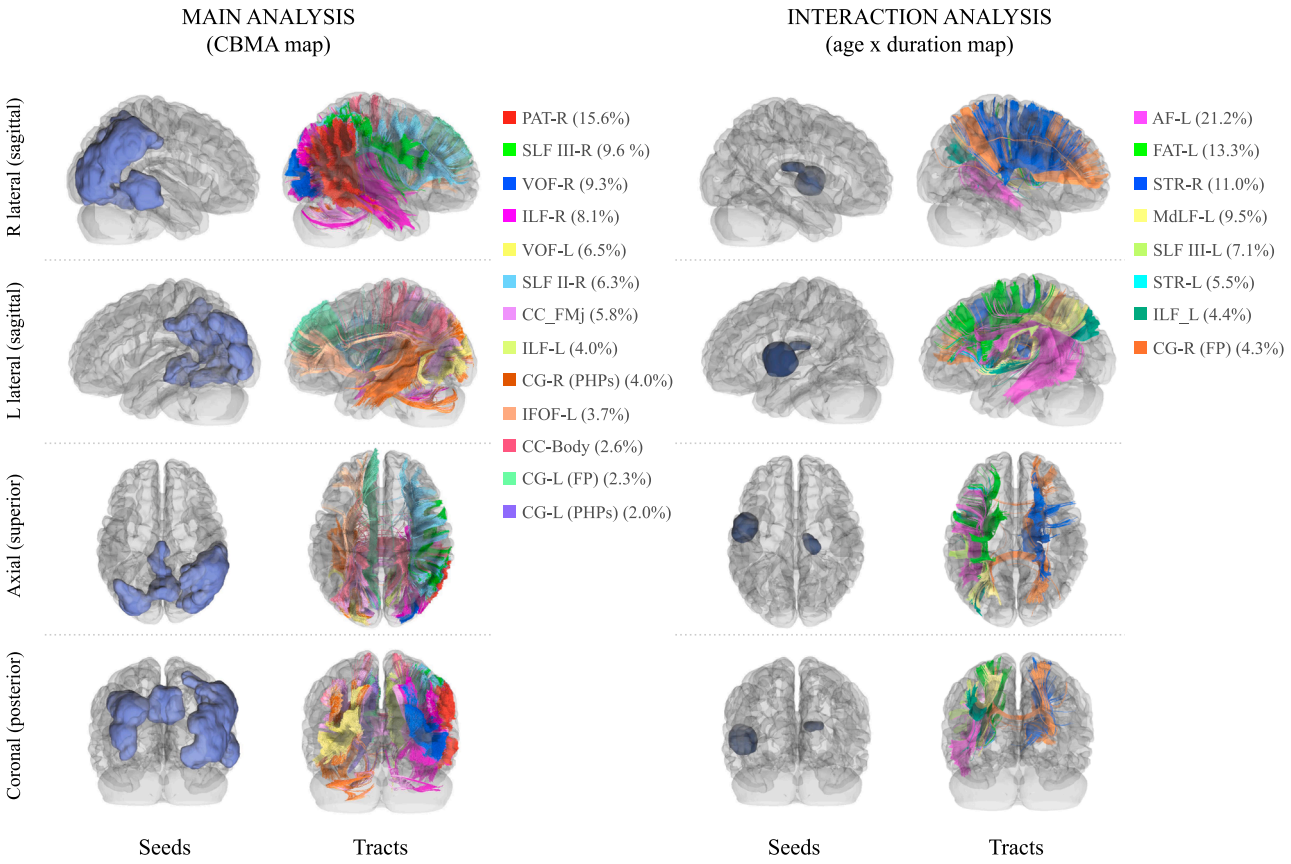

Fig. 5. Structural connectivity results based on meta-analysis and meta-regression atrophy maps. Tractography based on the HCP-1065 population-averaged diffusion template. The left panel shows tracts seeded from CBMA-derived atrophy regions, and the right panel those associated with the age × disease duration interaction. Axial, sagittal, and coronal views highlight the main color-coded white matter pathways intersecting the atrophic clusters, with labels indicating tract-specific streamline percentages. Acronyms: AF = Arcuate Fasciculus; CC-Body = Corpus Callosum - Body; CC-FMj = Corpus Callosum - forceps major; CG (FP) = Cingulum (Frontal-Parietal segment); CG (PHPs) = Cingulum (Parahippocampal-Parietal segment); FAT = Frontal Aslant Tract; IFOF = Inferior Fronto-occipital Fasciculus; ILF = Inferior Longitudinal Fasciculus; L = Left; MdLF = Middle Longitudinal Fasciculus; PAT = Parietal Aslant Tract; R = Right; SLF = Superior Longitudinal Fasciculus; STR = Superior thalamic radiations; VOF = Vertical Occipital Fasciculus.

contexts.

An important methodological advance of the present study is the incorporation of meta-regression analyses. A preliminary analysis revealed a strong negative correlation between mean age and disease duration across samples. This pattern likely reflects a characteristic feature of PCA, in which diagnosis is often delayed due to its presenile onset and atypical visual presentation, leading many patients to undergo multiple ophthalmological assessments before neurological referral (Balasa et al., 2011; Cogan, 1985; Crutch et al., 2017; Murray et al., 2011; Tang-Wai et al., 2004). Moreover, consistent with other early-onset AD phenotypes (Hammers et al., 2025), early-onset PCA has been reported to exhibit a faster clinical course and progression than late-onset PCA (Isella et al., 2022b; Phillips et al., 2021).

In the meta-regression analysis, while no significant associations were found for gender, education, or MMSE scores, we identified a significant interaction between age and disease duration, which was associated with atrophy in the left superior temporal gyrus and right thalamus. These findings suggest a possible age-by-duration modulation of neurodegeneration in PCA, with implications for language impairment (linked to left temporal regions) and functional decline (associated with right thalamic damage). Notably, this resonates with emerging clinical observations of language deficits in advanced PCA cases resembling logopenic PPA (Ahmed et al., 2024; Fitzpatrick et al., 2019; Magnin et al., 2013), and recent evidence linking thalamic atrophy to disease severity and autonomy loss in PCA (Wang et al., 2024).

Our tractography analyses provide a complementary perspective on the structural architecture potentially underlying the observed patterns of GM atrophy in PCA, highlighting WM pathways that may mediate or reflect disease-related network disconnection, as inferred within a normative-connectivity framework (Dogan et al., 2015; Jiang et al., 2023; Li et al., 2021; Liang et al., 2023; Phillips et al., 2019; Ravano et al., 2021; Salvalaggio et al., 2020; Smits et al., 2023).

The first connectivity analysis, seeding on composite seeding of the meta-analytic atrophy map, highlighted predominant involvement of the right PAT, SLF, and ILF, as well as the bilateral VOF, together with additional interhemispheric and associative bundles such as the corpus callosum, left IFOF, and cingulum. This pattern broadly aligns with the posterior-to-anterior disconnection profile previously described in PCA (Migliaccio et al., 2012a; Phillips et al., 2024), encompassing tracts that are crucial for visuospatial integration, as well as for functions supported by the dorsal and ventral visual streams and visuomotor coordination, all of which represent key domains impaired in PCA (Migliaccio et al., 2016, 2012b; Montembeault et al., 2018).

The second connectivity analysis, based on composite seeding of the age × disease-duration interaction map, revealed a left-lateralized pattern involving the AF, FAT, and bilateral STR. These tracts, associated with language and executive functions, may reflect compensatory or alternative disconnection pathways emerging in younger-onset, longer-duration cases. Consistent with left temporal involvement and logopenic-like features, the AF has been related to phonological and repetition processes (Breier et al., 2008), while the FAT has been linked to visuospatial and constructional abilities in AD (Serra et al., 2017). The STR may represent a key substrate of thalamo-cortical disconnection, whose involvement has been associated with greater disease severity

and executive dysfunction in AD (Doan et al., 2017; Niida et al., 2013; Wen et al., 2019).

The observed interaction supports the hypothesis of an additional right-to-left gradient of degeneration, complementing the widely described posterior-to-anterior trajectory in PCA. This dual-gradient model offers a unifying framework for interpreting earlier findings of predominant right-hemisphere disconnection (Cerami et al., 2015; Madhavan et al., 2016) and may help account for the clinical heterogeneity frequently seen in PCA. Future longitudinal studies are warranted to validate this hypothesis. Together, these tract-level findings offer a neuroanatomical framework linking posterior GM atrophy with long-range associative disconnection, consistent with emerging network-based models of AD (Hwang et al., 2019; Liang et al., 2023; Lombardi et al., 2020; Mongay-Ochoa et al., 2025; Palop and Mucke, 2016; Qing et al., 2021). They also reinforce the emerging view that PCA is not confined to degeneration of the visual cortex but involves broader disruption of large-scale networks (Agosta et al., 2018; Glick-Shames et al., 2020; Migliaccio et al., 2020; Phillips et al., 2024; Singh et al., 2024). The variable hemispheric distribution of affected tracts may reflect individual disease trajectories and could be modulated by the relationship between WM microstructural abnormalities and the expression of clinical symptoms (Millington et al., 2017).

This study has some limitations that should be acknowledged. Although this meta-analysis included the largest number of PCA studies to date, PCA remains a rare clinical syndrome, and the number of eligible whole-brain VBM datasets remains relatively limited compared to typical AD. Second, the absence of syndrome-specific cognitive measures (such as simultanagnosia tasks, complex figure copying, or comprehensive visuospatial and visuoperceptual test batteries) limits the specificity and interpretability of the meta-regression analysis. The reliance on MMSE as a general index of disease severity may be suboptimal, as this global cognitive screening tool is poorly sensitive to the posterior deficits that are characteristic of PCA. Moreover, disease duration was retrospectively estimated in most included studies, thereby introducing potential variability across cohorts. Finally, tractography was performed within a normative-connectivity framework projecting atrophy maps onto a population-averaged connectome. This approach enables reproducible and anatomically standardized inferences and mitigates potential false negatives that may arise when patient-specific WM degeneration compromises tractography (Phillips et al., 2019; Yeh et al., 2018). However, it does not capture individual variability, and the use of a young healthy template likely provides an upper-bound estimate of WM integrity, given the well-established age-related decline in WM microstructure (Bennett and Madden, 2013; Madden et al., 2012). Consequently, the inferred disconnection patterns should be interpreted as conservative, topographic indicators of pathways at risk, and may underestimate the actual extent of WM disruption in older PCA cohorts. Nonetheless, the high-quality HCP templates offer excellent spatial resolution and methodological reliability, and remain a valuable resource for exploratory indirect-mapping analyses (Liang et al., 2023; Phillips et al., 2019; Yeh et al., 2018).

Future research should prioritize the integration of multimodal neuroimaging techniques (including structural MRI, DTI, functional MRI, and PET) to identify converging biomarkers that can capture the complexity of disease progression and phenotypic variability in PCA. In this context, molecular PET imaging, particularly amyloid and tau PET, provides critical complementary information for assessing pathological burden, refining clinicopathological interpretation, and guiding longitudinal monitoring (Gan et al., 2025; Katsumi et al., 2025; La Joie et al., 2021; Phillips et al., 2021). Such approaches may enhance diagnostic accuracy and enable improved stratification of patients for targeted interventions. Additionally, longitudinal studies will be crucial to elucidate the temporal dynamics of GM and WM changes and their relationship with evolving cognitive and functional impairments, thereby improving our understanding of the mechanisms underlying disease progression and clinical heterogeneity in PCA.

Conclusion

This study provides the most comprehensive meta-analysis of VBM in PCA to date. Results demonstrate consistent GM loss in occipital, parietal, precuneus, and ventral temporal regions, and reveal an interaction between age and disease duration associated with temporal and thalamic involvement. These findings refine the neuroanatomical profile of PCA and underscore its distributed and asymmetric nature. Structural connectivity analyses further suggest posterior–anterior and right–left gradients of network disruption.

Together, these results advance the development of imaging biomarkers capable of improving early diagnosis, stratifying disease stages, and guiding therapeutic interventions. In particular, they highlight the potential for network-targeted approaches, including neuromodulation strategies. Future multimodal and longitudinal studies will be crucial to track disease progression, clarify the links between structural disconnection and cognitive decline, and support personalized clinical management in this heterogeneous and often under-recognized syndrome.

Declaration of Generative AI and AI-assisted technologies in the writing process

During the preparation of this work, the authors used ChatGPT (OpenAI) in order to assist in drafting and revising sections of the manuscript. After using this tool, the authors reviewed and edited the content as needed and take full responsibility for the content of the publication.

Funding

This research did not receive any specific grant from funding agencies in the public, commercial, or not-for-profit sectors.

Declaration of Competing Interest

The authors did not declare any conflict of interest.

Appendix A. Supporting information

Supplementary data associated with this article can be found in the online version at doi:10.1016/j.neubiorev.2026.106554.

Data availability

The data presented in this study, including the data extraction sheet and the statistical maps generated from the meta-analysis, will be made publicly available in an open-access repository upon publication. Until the dataset release, all relevant data can be obtained from the corresponding author upon reasonable request.

References

Agosta, F., Mandic-Stojmenovic, G., Canu, E., Stojkovic, T., Imperiale, F., Caso, F., Stefanova, E., Copetti, M., Kostic, V.S., Filippi, M., 2018. Functional and structural brain networks in Posterior Cortical Atrophy: a two-centre multiparametric MRI study. Neuroimage Clin. 19, 901. https://doi.org/10.1016/J.NICL.2018.06.013.

Ahmed, S., Loane, C., Bartels, S., Zamboni, G., Mackay, C., Baker, I., Husain, M., Thompson, S., Hornberger, M., Butler, C., 2018. Lateral parietal contributions to memory impairment in Posterior Cortical Atrophy. Neuroimage Clin. 20, 252. https://doi.org/10.1016/J.NICL.2018.07.005.

Ahmed, S., Culley, S., Blanco-Duque, C., Hodges, J.R., Butler, C., Mioshi, E., 2020. Pronounced impairment of activities of daily living in Posterior Cortical Atrophy. Dement Geriatr. Cogn. Disord. 49, 48–55. https://doi.org/10.1159/000506125.

Ahmed, S., Caswell, J., Butler, C.R., Bose, A., Sintini, I., Putcha, D., Marshall, C., 2024. Secondary language impairment in posterior cortical atrophy: insights from sentence repetition. Front Neurosci. 18, 1359186. https://doi.org/10.3389/FNINS.2024.1359186.

Albajes-Eizagirre, A., Solanes, A., Fullana, M.A., Ioannidis, J.P.A., Fusar-Poli, P., Torrent, C., Solé, B., Bonnín, C.M., Vieta, E., Mataix-Cols, D., Radua, J., 2019a. Meta-analysis of Voxel-Based Neuroimaging Studies using Seed-based d Mapping with

Permutation of Subject Images (SDM-PSI. JoVE J. Vis. Exp. 2019, e59841. https://doi.org/10.3791/59841.
Albajes-Eizagirre, A., Solanes, A., Radua, J., 2019b. Meta-analysis of non-statistically significant unreported effects. Stat. Methods Med. Res. 28, 3741–3754. https://doi.org/10.1177/0962280218811349.
Albajes-Eizagirre, A., Solanes, A., Vieta, E., Radua, J., 2019c. Voxel-based meta-analysis via permutation of subject images (PSI): theory and implementation for SDM. Neuroimage 186, 174–184. https://doi.org/10.1016/j.neuroimage.2018.10.077.
Alves, J., Soares, J.M., Sampaio, A., Gonçalves, Ó.F., 2013. Posterior cortical atrophy and Alzheimer's disease: a meta-analytic review of neuropsychological and brain morphometry studies. Brain Imaging Behav. 7, 353–361. https://doi.org/10.1007/S11682-013-9236-1.
Balasa, M., Gelpi, E., Antonell, A., Rey, M.J., Sánchez-Valle, R., Molinuevo, J.L., Lladó, A., 2011. Clinical features and APOE genotype of pathologically proven early-onset Alzheimer disease. Neurology 76, 1720–1725. https://doi.org/10.1212/WNL.0b013e31821a44dd.
Bennett, I.J., Madden, D.J., 2013. Disconnected aging: cerebral white matter integrity and age-related differences in cognition. Neuroscience 0 187. https://doi.org/10.1016/J.NEUROSCIENCE.2013.11.026.
Benson, D.F., Davis, R.J., Snyder, B.D., 1988. Posterior Cortical Atrophy. Arch. Neurol. 45, 789–793. https://doi.org/10.1001/archneur.1988.00520310107024.
Best, J., Chapleau, M., Rabinovici, G.D., 2023. Posterior cortical atrophy: clinical, neuroimaging, and neuropathological features. Expert Rev. Neurother. 23, 227–236. https://doi.org/10.1080/14737175.2023.2190885.
Breier, J.I., Hasan, K.M., Zhang, W., Men, D., Papanicolaou, A.C., 2008. Language dysfunction after stroke and damage to white matter tracts evaluated using diffusion tensor imaging. AJNR Am. J. Neuroradiol. 29, 483–487. https://doi.org/10.3174/AJNR.A0846.
Cerami, C., Crespi, C., Della Rosa, P.A., Dodich, A., Marcone, A., Magnani, G., Coppi, E., Falini, A., Cappa, S.F., Perani, D., 2015. Brain changes within the visuo-spatial attentional network in posterior cortical atrophy. J. Alzheimer'S Dis. 43, 385–395. https://doi.org/10.3233/JAD-141275.
Chapleau, M., La Joie, R., Yong, K., Agosta, F., Allen, I.E., Apostolova, L., Best, J., Boon, B.D.C., Crutch, S., Filippi, M., Fumagalli, G.G., Galimberti, D., Graff-Radford, J., Grinberg, L.T., Irwin, D.J., Josephs, K.A., Mendez, M.F., Mendez, P.C., Migliaccio, R., Miller, Z.A., Montembeault, M., Murray, M.E., Nemes, S., Pelak, V., Perani, D., Phillips, J., Pijnenburg, Y., Rogalski, E., Schott, J.M., Seeley, W., Sullivan, A.C., Spina, S., Tanner, J., Walker, J., Whitwell, J.L., Wolk, D.A., Ossenkoppele, R., Rabinovici, G.D., Abdi, Z., Ahmed, S., Alcolea, D., Allinson, K.S.J., Arighi, A., Balasa, M., Barkhof, F., Brandt, K.D., Brosch, J., Burrell, J., Butler, C.R., Calandri, I., Caminiti, S.P., Canu, E., Carrillo, M.C., Caso, F., Chu, M., Cordato, N., Costa, A.S., Cui, Y., Dickerson, B., Dickson, D.W., Duara, R., Dubois, B., Eldaief, M., Farlow, M., Feneglio, C., Fliessbach, K., Formaglio, M., Fortea, J., Fox, N., Foxe, D., Tilikete, C.F., Frosch, M.P., Galasko, D., Garat, O., Giardinieri, G., Graff-Radford, N. R., Groot, C., Hake, A.M., Hansson, O., Headley, A., Hernandez, M., Hochberg, D., Hodges, J.R., Hof, P.R., Holton, J., Hromas, G., Illán Gala, I., Jaunmuktane, Z., Jing, D., Kagerer, S.M., Kasuga, K., Kong, Y., Kövari, E., Lacombe-Thibault, M., Lleó Plarrumaní, A., Lucente, D.E., Machulda, M.M., Magnani, G., Magnin, E., Malpetti, M., Matthews, B., McGinnis, S., Mesulam, M., Miklitz, C., Mundada, N., Nestor, P.J., Ocal, D., Paterson, R., Piguet, O., Putcha, D., Quimby, M., Reetz, K., Rein, N., Revesz, T., Rezaii, N., Rodriguez-Porcel, F., Rowe, J.B., Ryan, N., Sanchez-Valle, R., Sacchi, L., Santos-Santos, M.Á., Sherman, J., Stomrud, E., Tideman, P., Tokutake, T., Tondo, G., Touroutoglou, A., Tousi, B., Vandenberghe, R., van der Flier, W., Weintraub, S., Wong, B., Wu, L., Xie, K., 2024. Demographic, clinical, biomarker and neuropathologic correlates in Posterior Cortical Atrophy: an individual participant data meta-analysis. Lancet Neurol. 23, 168. https://doi.org/10.1016/S1474-4422(23)00414-3.
Clark, J.M., Sanders, S., Carter, M., Honeyman, D., Cleo, G., Auld, Y., Booth, D., Condron, P., Dalais, C., Bateup, S., Linthwaite, B., May, N., Munn, J., Ramsay, L., Rickett, K., Rutter, C., Smith, A., Sondergeld, P., Wallin, M., Jones, M., Beller, E., 2020. Improving the translation of search strategies using the Polyglot Search Translator: a randomized controlled trial. J. Med. Libr Assoc. 108, 195–207. https://doi.org/10.5195/JMLA.2020.834.
Cogan, D.G., 1985. Visual disturbances with focal progressive dementing disease. Am. J. Ophthalmol. 100, 68–72. https://doi.org/10.1016/S0002-9394(14)74985-2.
Cope, T.E., Hughes, L.E., Phillips, H.N., Adams, N.E., Jafarian, A., Nesbitt, D., Assem, M., Woolgar, A., Duncan, J., Rowe, J.B., 2022. Causal evidence for the multiple demand network in change detection: auditory mismatch magnetoencephalography across focal neurodegenerative diseases. J. Neurosci. 42, 3197–3215. https://doi.org/10.1523/JNEUROSCI.1622-21.2022.
Crane, P.K., Groot, C., Ossenkoppele, R., Mukherjee, S., Choi, S.E., Lee, M., Scollard, P., Gibbons, L.E., Sanders, R.E., Trittschuh, E., Saykin, A.J., Mez, J., Nakano, C., Donald, C.Mac, Sohi, H., Risacher, S., 2024. Cognitively defined Alzheimer's dementia subgroups have distinct atrophy patterns. Alzheimer'S. Dement. 20, 1739–1752. https://doi.org/10.1002/ALZ.13567.
Crutch, S.J., Lehmann, M., Schott, J.M., Rabinovici, G.D., Rossor, M.N., Fox, N.C., 2012. Posterior cortical atrophy. Lancet Neurol. https://doi.org/10.1016/S1474-4422(11)70289-7.
Crutch, S.J., Schott, J.M., Rabinovici, G.D., Murray, M., Snowden, J.S., van der Flier, W. M., Dickerson, B.C., Vandenberghe, R., Ahmed, S., Bak, T.H., Boeve, B.F., Butler, C., Cappa, S.F., Ceccaldi, M., Cruz de Souza, L., Dubois, B., Felician, O., Galasko, D., Graff-Radford, J., Graff-Radford, N.R., Hof, P.R., Krolak-Salmon, P., Lehmann, M., Magnin, E., Mendez, M.F., Nestor, P.J., Onyike aa, C.U., Pelak bb, V.S., Pijnenburg, Y., Primativo, S., Rossor, M.N., Ryan, N.S., Scheltens, P., Shakespeare, T. J., Suárez González, A., Tang-Wai ee, D.F., X Yong, K.X., Carrillo ff, M., Fox, N.C., Lyon, of, Yong, K.X.X., Fox, N.C., Rabinovici, G.D., Lehmann, M., Murray, M., Snowden, J.S., Snowden, J.S., van der Flier, W.M., Pijnenburg, Y., Scheltens, P., van der Flier, W.M., Pijnenburg, Y., Scheltens, P., Dickerson, B.C., Vandenberghe, R., Ahmed, S., Butler, C., Bak, T.H., Boeve, B.F., Graff-Radford, J., Cappa, S.F., Ceccaldi, M., de Souza, L.C., Dubois, B., Felician, O., Felician, O., Galasko, D., Graff-Radford, N.R., Hof, P.R., Hof, P.R., Krolak-Salmon, P., Magnin, E., Mendez, M.F., Nestor, P.J., Onyike, C.U., Pelak, V.S., Suárez González, A., Tang-Wai, D. F., Carrillo, M., 2017. Consensus classification of Posterior Cortical Atrophy. Alzheimer'S Dement. 13, 870–884. https://doi.org/10.1016/j.jalz.2017.01.014.
Cui, Y., Liu, Y., Yang, C., Cui, C., Jing, D., Zhang, X., Chen, Y., Li, B., Liang, Z., Chen, K., Zhang, Z., Wu, L., 2022. Brain structural and functional anomalies associated with simultanagnosia in patients with Posterior Cortical Atrophy. Brain Imaging Behav. 16, 1148–1162. https://doi.org/10.1007/S11682-021-00568-8.
Doan, N.T., Engvig, A., Persson, K., Alnæs, D., Kaufmann, T., Rokicki, J., Córdova-Palomera, A., Moberget, T., Brækhus, A., Barca, M.L., Engedal, K., Andreassen, O.A., Selbæk, G., Westlye, L.T., 2017. Dissociable diffusion MRI patterns of white matter microstructure and connectivity in Alzheimer's disease spectrum. Sci. Rep. 1–12. https://doi.org/10.1038/srep45131.
Dogan, I., Eickhoff, C.R., Fox, P.T., Laird, A.R., Schulz, J.B., Eickhoff, S.B., Reetz, K., 2015. Functional connectivity modeling of consistent cortico-striatal degeneration in Huntington's disease. Neuroimage Clin. 7, 640. https://doi.org/10.1016/J.NICL.2015.02.018.
Dubois, B., Feldman, H.H., Jacova, C., Hampel, H., Molinuevo, J.L., Blennow, K., Dekosky, S.T., Gauthier, S., Selkoe, D., Bateman, R., Cappa, S., Crutch, S., Engelborghs, S., Frisoni, G.B., Fox, N.C., Galasko, D., Habert, M.O., Jicha, G.A., Nordberg, A., Pasquier, F., Rabinovici, G., Robert, P., Rowe, C., Salloway, S., Sarazin, M., Epelbaum, S., de Souza, L.C., Vellas, B., Visser, P.J., Schneider, L., Stern, Y., Scheltens, P., Cummings, J.L., 2014. Advancing research diagnostic criteria for Alzheimer's disease: the IWG-2 criteria. Lancet Neurol. 13, 614–629. https://doi.org/10.1016/S1474-4422(14)70090-0.
Egger, M., Smith, G.D., Schneider, M., Minder, C., 1997. Bias in meta-analysis detected by a simple, graphical test. BMJ 315, 629–634. https://doi.org/10.1136/BMJ.315.7109.629.
Eickhoff, S.B., Bzdok, D., Laird, A.R., Roski, C., Caspers, S., Zilles, K., Fox, P.T., 2011. Co-activation patterns distinguish cortical modules, their connectivity and functional differentiation. Neuroimage 57, 938–949. https://doi.org/10.1016/J.NEUROIMAGE.2011.05.021.
Fitzpatrick, D., Blanco-Campal, A., Kyne, L., 2019. A Case of overlap Posterior Cortical Atrophy and logopenic variant primary progressive aphasia. Neurologist 24, 62–65. https://doi.org/10.1097/NRL.0000000000000225.
Fredericks, C.A., Brown, J.A., Deng, J., Kramer, A., Ossenkoppele, R., Rankin, K., Kramer, J.H., Miller, B.L., Rabinovici, G.D., Seeley, W.W., 2019. Intrinsic connectivity networks in Posterior Cortical Atrophy: a role for the pulvinar? Neuroimage Clin. 21, 101628. https://doi.org/10.1016/j.nicl.2018.101628.
Fumagalli, G.G., Basilico, P., Arighi, A., Mercurio, M., Scarioni, M., Carandini, T., Colombi, A., Pietroboni, A.M., Sacchi, L., Conte, G., Scola, E., Triulzi, F., Scarpini, E., Galimberti, D., 2020. Parieto-occipital sulcus widening differentiates Posterior Cortical Atrophy from typical Alzheimer disease. Neuroimage Clin. 28. https://doi.org/10.1016/j.nicl.2020.102453.
Gan, R., Xie, H., Zhao, Z., Wu, X., Wang, R., Wu, B., Chen, Q., Jia, Z., 2025. Investigation of patterns and associations of neuroinflammation in cognitive impairment. Cereb. Cortex 35. https://doi.org/10.1093/CERCOR/BHAF013.
Glasser, M.F., Sotiropoulos, S.N., Wilson, J.A., Coalson, T.S., Fischl, B., Andersson, J.L., Xu, J., Jbabdi, S., Webster, M., Polimeni, J.R., Van Essen, D.C., Jenkinson, M., 2013. The minimal preprocessing pipelines for the Human Connectome Project. Neuroimage 80, 105–124. https://doi.org/10.1016/j.neuroimage.2013.04.127.
Glick-Shames, H., Backner, Y., Bick, A., Raz, N., Levin, N., 2019. The impact of localized grey matter damage on neighboring connectivity: Posterior Cortical Atrophy and the visual network. Brain Imaging Behav. 13, 1292–1301. https://doi.org/10.1007/S11682-018-9952-7.
Glick-Shames, H., Keadan, T., Backner, Y., Bick, A., Levin, N., 2020. Global brain involvement in Posterior Cortical Atrophy: multimodal MR imaging investigation. Brain Topogr. 33, 600–612. https://doi.org/10.1007/S10548-020-00788-Z.
Grady, C.L., Rieck, J.R., Nichol, D., Rodrigue, K.M., Kennedy, K.M., 2021. Influence of sample size and analytic approach on stability and interpretation of brain-behavior correlations in task-related fMRI data. Hum. Brain Mapp. 42, 204–219. https://doi.org/10.1002/HBM.25217.
Hammers, D.B., Eloyan, A., Thangarajah, M., Taurone, A., Beckett, L., Gao, S., Polsinelli, A.J., Kirby, K., Dage, J.L., Nudelman, K., Aisen, P., Reman, R., La Joie, R., Lagarde, J., Atri, A., Clark, D., Day, G.S., Duara, R., Graff-Radford, N.R., Honig, L.S., Jones, D.T., Masdeu, J.C., Mendez, M.F., Womack, K., Musiek, E., Onyike, C.U., Riddle, M., Grant, I., Rogalski, E., Johnson, E.C.B., Salloway, S., Sha, S.J., Turner, R. S., Wingo, T.S., Wolk, D.A., Carrillo, M.C., Dickerson, B.C., Rabinovici, G.D., Apostolova, L.G., 2025. Differences in baseline cognitive performance between participants with early-onset and late-onset Alzheimer's disease: comparison of LEADS and ADNI. Alzheimers Dement 21. https://doi.org/10.1002/ALZ.14218.
Higgins, J.P.T., Thompson, S.G., Deeks, J.J., Altman, D.G., 2003. Measuring inconsistency in meta-analyses. BMJ Br. Med. J. 327, 557. https://doi.org/10.1136/BMJ.327.7414.557.
Hwang, S.J., Adluru, N., Kim, W.H., Johnson, S.C., Bendlin, B.B., Singh, V., 2019. Associations between positron emission tomography amyloid pathology and diffusion tensor imaging brain connectivity in pre-clinical Alzheimer's disease. Brain Connect 9, 162–173. https://doi.org/10.1089/BRAIN.2018.0590.
Isella, V., Licciardo, D., Nastasi, G., Impagnatiello, V., Ferri, F., Mapelli, C., Crivellaro, C., Musarra, M., Morzenti, S., Appollonio, I., Ferrarese, C., 2022b. Clinical and metabolic imaging features of late-onset and early-onset Posterior Cortical Atrophy. Eur. J. Neurol. 29, 3147–3157. https://doi.org/10.1111/ene.15520.

Isella, V., Crivellaro, C., Formenti, A., Musarra, M., Pacella, S., Morzenti, S., Ferri, F., Mapelli, C., Gallivanone, F., Guerra, L., Appollonio, I., Ferrarese, C., 2022a. Validity of cingulate–precuneus–temporo-parietal hypometabolism for single-subject diagnosis of biomarker-proven atypical variants of Alzheimer's Disease. J. Neurol. 269, 4440–4451. https://doi.org/10.1007/s00415-022-11086-y.

Jiang, J., Bruss, J., Lee, W.T., Tranel, D., Boes, A.D., 2023. White matter disconnection of left multiple demand network is associated with post-lesion deficits in cognitive control. Nat. Commun. 14, 1740. https://doi.org/10.1038/S41467-023-37330-1.

Katsumi, Y., Howe, I.A., Eckbo, R., Wong, B., Quimby, M., Hochberg, D., McGinnis, S.M., Putcha, D., Wolk, D.A., Touroutoglou, A., Dickerson, B.C., 2025. Default mode network tau predicts future clinical decline in atypical early Alzheimer's disease. Brain 148, 1329–1344. https://doi.org/10.1093/BRAIN/AWAE327.

Koch, G., Bonnì, S., Pellicciari, M.C., Casula, E.P., Mancini, M., Esposito, R., Ponzo, V., Picazio, S., Di Lorenzo, F., Serra, L., Motta, C., Maiella, M., Marra, C., Cercignani, M., Martorana, A., Caltagirone, C., Bozzali, M., 2018. Transcranial magnetic stimulation of the precuneus enhances memory and neural activity in prodromal Alzheimer's disease. Neuroimage 169, 302–311. https://doi.org/10.1016/j.neuroimage.2017.12.048.

Koch, G., Casula, E.P., Bonnì, S., Borghi, I., Assogna, M., Minei, M., Pellicciari, M.C., Motta, C., D'Acunto, A., Porrazzini, F., Maiella, M., Ferrari, C., Caltagirone, C., Santarnecchi, E., Bozzali, M., Martorana, A., 2022. Precuneus magnetic stimulation for Alzheimer's disease: a randomized, sham-controlled trial. Brain 145, 3776–3786. https://doi.org/10.1093/BRAIN/AWAC285.

Koedam, E.L.G.E., Lauffer, V., Van Der Vlies, A.E., Van Der Flier, W.M., Scheltens, P., Pijnenburg, Y.A.L., 2010. Early-versus late-onset Alzheimer's disease: More than age alone. J. Alzheimer'S Dis. 19, 1401–1408. https://doi.org/10.3233/JAD-2010-1337.

La Joie, R., Visani, A.V., Lesman-Segev, O.H., Baker, S.L., Edwards, L., Iaccarino, L., Soleimani-Meigooni, D.N., Mellinger, T., Janabi, M., Miller, Z.A., Perry, D.C., Pham, J., Strom, A., Gorno-Tempini, M.L., Rosen, H.J., Miller, B.L., Jagust, W.J., Rabinovici, G.D., 2021. Association of APOE4 and clinical variability in Alzheimer disease with the pattern of tau- and amyloid-PET. Neurology 96, e650. https://doi.org/10.1212/WNL.0000000000011270.

Lehmann, M., Crutch, S.J., Ridgway, G.R., Ridha, B.H., Barnes, J., Warrington, E.K., Rossor, M.N., Fox, N.C., 2011. Cortical thickness and voxel-based morphometry in Posterior Cortical Atrophy and typical Alzheimer's disease. Neurobiol. Aging 32, 1466–1476. https://doi.org/10.1016/j.neurobiolaging.2009.08.017.

Li, Z., Dolui, S., Habes, M., Bassett, D.S., Wolk, D., Detre, J.A., 2021. Predicted disconnectome associated with progressive periventricular white matter ischemia. Cereb. Circ. Cogn. Behav. 2, 100022. https://doi.org/10.1016/J.CCCB.2021.100022.

Liang, L., Zhou, P., Ye, C., Yang, Q., Ma, T., 2023. Spatial-temporal patterns of brain disconnectome in Alzheimer's disease. Hum. Brain Mapp. 44, 4272–4286. https://doi.org/10.1002/HBM.26344.

Liberati, A., Altman, D.G., Tetzlaff, J., Mulrow, C., Gøtzsche, P.C., Ioannidis, J.P.A., Clarke, M., Devereaux, P.J., Kleijnen, J., Moher, D., 2009. The PRISMA statement for reporting systematic reviews and meta-analyses of studies that evaluate healthcare interventions: explanation and elaboration. BMJ 339, b2700. https://doi.org/10.1136/bmj.b2700.

Lombardi, A., Amoroso, N., Diacono, D., Monaco, A., Logroscino, G., De Blasi, R., Bellotti, R., Tangaro, S., 2020. Association between structural connectivity and generalized cognitive spectrum in alzheimer's disease. Brain Sci. 10, 1–17. https://doi.org/10.3390/BRAINSCI10110879.

Madden, D.J., Bennett, I.J., Burzynska, A., Potter, G.G., Chen, N. kuei, Song, A.W., 2012. Diffusion tensor imaging of cerebral white matter integrity in cognitive aging. Biochim. Et. Biophys. Acta (BBA) Mol. Basis Dis. 1822, 386–400. https://doi.org/10.1016/J.BBADIS.2011.08.003.

Madhavan, A., Schwarz, C.G., Duffy, J.R., Strand, E.A., Machulda, M.M., Drubach, D.A., Kantarci, K., Przybelski, S.A., Reid, R.I., Senjem, M.L., Gunter, J.L., Apostolova, L.G., Lowe, V.J., Petersen, R.C., Jack, C.R., Josephs, K.A., Whitwell, J.L., 2016. Characterizing white matter tract degeneration in syndromic variants of Alzheimer's disease: a diffusion tensor imaging study. J. Alzheimers Dis. 49, 633. https://doi.org/10.3233/JAD-150502.

Magnin, E., Sylvestre, G., Lenoir, F., Dariel, E., Bonnet, L., Chopard, G., Tio, G., Hidalgo, J., Ferreira, S., Mertz, C., Binetruy, M., Chamard, L., Haffen, S., Ryff, I., Laurent, E., Moulin, T., Vandel, P., Rumbach, L., 2013. Logopenic syndrome in Posterior Cortical Atrophy. J. Neurol. 260, 528–533. https://doi.org/10.1007/s00415-012-6671-7.

McKhann, G.M., Knopman, D.S., Chertkow, H., Hyman, B.T., Jack, C.R., Kawas, C.H., Klunk, W.E., Koroshetz, W.J., Manly, J.J., Mayeux, R., Mohs, R.C., Morris, J.C., Rossor, M.N., Scheltens, P., Carrillo, M.C., Thies, B., Weintraub, S., Phelps, C.H., 2011. The diagnosis of dementia due to Alzheimer's disease: recommendations from the National Institute on Aging-Alzheimer's Association workgroups on diagnostic guidelines for Alzheimer's disease. Alzheimer's Dement. 7, 263–269. https://doi.org/10.1016/j.jalz.2011.03.005.

Menardi, A., Rossi, S., Koch, G., Hampel, H., Vergallo, A., Nitsche, M.A., Stern, Y., Borroni, B., Cappa, S.F., Cotelli, M., Ruffini, G., El-Fakhri, G., Rossini, P.M., Dickerson, B., Antal, A., Babiloni, C., Lefaucheur, J.P., Dubois, B., Deco, G., Ziemann, U., Pascual-Leone, A., Santarnecchi, E., 2021. Toward noninvasive brain stimulation 2.0 in Alzheimer's disease. Ageing Res. Rev. 75, 101555. https://doi.org/10.1016/J.ARR.2021.101555.

Miettinen, K., 2003. Graphical illustration of pareto optimal solutions. MultiObject. Program. Goal Program. 197–202. https://doi.org/10.1007/978-3-540-36510-5_27.

Migliaccio, R., Agosta, F., Rascovsky, K., Karydas, A., Bonasera, S., Rabinovici, G.D., Miller, B.L., Gorno-Tempini, M.L., 2009. Clinical syndromes associated with posterior atrophy: early age at onset AD spectrum. Neurology 73, 1571–1578. https://doi.org/10.1212/WNL.0b013e3181c0d427.

Migliaccio, R., Agosta, F., Scola, E., Magnani, G., Cappa, S.F., Pagani, E., Canu, E., Comi, G., Falini, A., Gorno-Tempini, M.L., Bartolomeo, P., Filippi, M., 2012b. Ventral and dorsal visual streams in Posterior Cortical Atrophy: a DT MRI study. Neurobiol. Aging 33, 2572–2584. https://doi.org/10.1016/j.neurobiolaging.2011.12.025.

Migliaccio, R., Agosta, F., Possin, K.L., Rabinovici, G.D., Miller, B.L., Gorno-Tempini, M. L., 2012a. White matter atrophy in Alzheimer's disease variants. Alzheimer'S Dement. 8, S78. https://doi.org/10.1016/j.jalz.2012.04.010.

Migliaccio, R., Gallea, C., Kas, A., Perlbarg, V., Samri, D., Trotta, L., Michon, A., Lacomblez, L., Dubois, B., Lehericy, S., Bartolomeo, P., 2016. Functional connectivity of ventral and dorsal visual streams in Posterior Cortical Atrophy. J. Alzheimer'S Dis. 51, 1119–1130. https://doi.org/10.3233/JAD-150934.

Migliaccio, R., Agosta, F., Basaia, S., Cividini, C., Habert, M.O., Kas, A., Montembeault, M., Filippi, M., 2020. Functional brain connectome in Posterior Cortical Atrophy. Neuroimage Clin. 25. https://doi.org/10.1016/j.nicl.2019.102100.

Miller, Z.A., Rosenberg, L., Santos-Santos, M.A., Stephens, M., Allen, I.E., Isabel Hubbard, H., Cantwell, A., Mandelli, M.L., Grinberg, L.T., Seeley, W.W., Miller, B.L., Rabinovici, G.D., Gorno-Tempini, M.L., 2018. Prevalence of mathematical and visuospatial learning disabilities in patients with Posterior Cortical Atrophy. JAMA Neurol. 75, 728–737. https://doi.org/10.1001/JAMANEUROL.2018.0395.

Millington, R.S., James-Galton, M., Maia Da Silva, M.N., Plant, G.T., Bridge, H., 2017. Lateralized occipital degeneration in Posterior Cortical Atrophy predicts visual field deficits. Neuroimage Clin. 14, 242. https://doi.org/10.1016/J.NICL.2017.01.012.

Mongay-Ochoa, N., Gonzalez-Escamilla, G., Fleischer, V., Pareto, D., Rovira, À., Sastre-Garriga, J., Groppa, S., 2025. Structural covariance analysis for neurodegenerative and neuroinflammatory brain disorders. Brain 148, 3072–3084. https://doi.org/10.1093/BRAIN/AWAF151.

Montembeault, M., Brambati, S.M., Lamari, F., Michon, A., Samri, D., Epelbaum, S., Lacomblez, L., Lehéricy, S., Habert, M.O., Dubois, B., Kas, A., Migliaccio, R., 2018. Atrophy, metabolism and cognition in the posterior cortical atrophy spectrum based on Alzheimer's disease cerebrospinal fluid biomarkers. Neuroimage Clin. 20, 1018–1025. https://doi.org/10.1016/j.nicl.2018.10.010.

Müller, V.I., Cieslik, E.C., Laird, A.R., Fox, P.T., Radua, J., Mataix-Cols, D., Tench, C.R., Yarkoni, T., Nichols, T.E., Turkeltaub, P.E., Wager, T.D., Eickhoff, S.B., 2017. Ten simple rules for neuroimaging meta-analysis. Neurosci. Biobehav Rev. 84, 151. https://doi.org/10.1016/J.NEUBIOREV.2017.11.012.

Murray, M.E., Graff-Radford, N.R., Ross, O.A., Petersen, R.C., Duara, R., Dickson, D.W., 2011. Neuropathologically defined subtypes of Alzheimer's disease with distinct clinical characteristics: a retrospective study. Lancet Neurol. 10, 785–796. https://doi.org/10.1016/S1474-4422(11)70156-9.

Neitzel, J., Ortner, M., Haupt, M., Redel, P., Grimmer, T., Yakushev, I., Drzezga, A., Bublak, P., Preul, C., Sorg, C., Finke, K., 2016. Neuro-cognitive mechanisms of simultanagnosia in patients with posterior cortical atrophy. Brain 139, 3267–3280.

Niida, A., Niida, R., Kuniyoshi, K., Motomura, M., Uechi, A., 2013. Usefulness of visual evaluation of the anterior thalamic radiation by diffusion tensor tractography for differentiating between Alzheimer's disease and elderly major depressive disorder patients. Int. J. Gen. Med. 189. https://doi.org/10.2147/IJGM.S42953.

Otsu, N., 1979. Threshold selection method from gray-level histograms. IEEE Trans. Syst. Man Cyber SMC 9, 62–66. https://doi.org/10.1109/TSMC.1979.4310076.

Palop, J.J., Mucke, L., 2016. Network abnormalities and interneuron dysfunction in Alzheimer disease. Nat. Rev. Neurosci. 17, 777–792. https://doi.org/10.1038/NRN.2016.141.

Phillips, J.S., Da Re, F., Irwin, D.J., McMillan, C.T., Vaishnavi, S.N., Xie, S.X., Lee, E.B., Cook, P.A., Gee, J.C., Shaw, L.M., Trojanowski, J.Q., Wolk, D.A., Grossman, M., 2019. Longitudinal progression of grey matter atrophy in non-amnestic Alzheimer's disease. Brain 142, 1701–1722. https://doi.org/10.1093/BRAIN/AWZ091.

Phillips, J.S., Nitchie, F.J., Da Re, F., Olm, C.A., Cook, P.A., McMillan, C.T., Irwin, D.J., Gee, J.C., Dubroff, J.G., Grossman, M., Nasrallah, I.M., 2021. Rates of longitudinal change in 18F-flortaucipir PET vary by brain region, cognitive impairment, and age in atypicalAlzheimer's disease18Alzheimer's & Dementia123510.1002/ALZ.12456.

Phillips, J.S., Adluru, N., Chung, M.K., Radhakrishnan, H., Olm, C.A., Cook, P.A., Gee, J. C., Cousins, K.A.Q., Arezoumandan, S., Wolk, D.A., McMillan, C.T., Grossman, M., Irwin, D.J., 2024. Greater white matter degeneration and lower structural connectivity in non-amnestic vs. amnestic Alzheimer's disease. Front Neurosci. 18, 1353306. https://doi.org/10.3389/FNINS.2024.1353306.

Qing, Z., Chen, F., Lu, J., Lv, P., Li, W., Liang, X., Wang, M., Wang, Z., Zhang, X., Zhang, B., 2021. Causal structural covariance network revealing atrophy progression in Alzheimer's disease continuum. Hum. Brain Mapp. 42, 3950–3962. https://doi.org/10.1002/HBM.25531.

Radua, J., Mataix-Cols, D., 2009. Voxel-wise meta-analysis of grey matter changes in obsessive–compulsive disorder. Br. J. Psychiatry 195, 393–402. https://doi.org/10.1192/BJP.BP.108.055046.

Radua, J., Mataix-Cols, D., Phillips, M.L., El-Hage, W., Kronhaus, D.M., Cardoner, N., Surguladze, S., 2012. A new meta-analytic method for neuroimaging studies that combines reported peak coordinates and statistical parametric maps. Eur. Psychiatry 27, 605–611. https://doi.org/10.1016/J.EURPSY.2011.04.001.

Radua, J., Rubia, K., Canales-Rodríguez, E.J., Pomarol-Clotet, E., Fusar-Poli, P., Mataix-Cols, D., 2014. Anisotropic kernels for coordinate-based meta-analyses of neuroimaging studies. Front Psychiatry 5, 74823. https://doi.org/10.3389/FPSYT.2014.00013.

Ramanan, S., Alaeddin, S., Goldberg, Z. lee, Strikwerda-Brown, C., Hodges, J.R., Irish, M., 2018. Exploring the contribution of visual imagery to scene construction – evidence from Posterior Cortical Atrophy. Cortex 106, 261–274. https://doi.org/10.1016/j.cortex.2018.06.016.

Ranasinghe, K.G., Hinkley, L.B., Beagle, A.J., Mizuiri, D., Dowling, A.F., Honma, S.M., Finucane, M.M., Scherling, C., Miller, B.L., Nagarajan, S.S., Vossel, K.A., 2014.

Regional functional connectivity predicts distinct cognitive impairments in Alzheimer's disease spectrum. Neuroimage Clin. 5, 385–395. https://doi.org/10.1016/j.nicl.2014.07.006.

Ravano, V., Andelova, M., Fartaria, M.J., Mahdi, M.F.A.W., Maréchal, B., Meuli, R., Uher, T., Krasensky, J., Vaneckova, M., Horakova, D., Kober, T., Richiardi, J., 2021. Validating atlas-based lesion disconnectomics in multiple sclerosis: a retrospective multi-centric study. Neuroimage Clin. 32, 102817. https://doi.org/10.1016/J.NICL.2021.102817.

Ryan, N.S., Shakespeare, T.J., Lehmann, M., Keihaninejad, S., Nicholas, J.M., Leung, K. K., Fox, N.C., Crutch, S.J., 2014. Motor features in Posterior Cortical Atrophy and their imaging correlates. Neurobiol. Aging 35, 2845–2857. https://doi.org/10.1016/j.neurobiolaging.2014.05.028.

Salvalaggio, A., de Filippo De Grazia, M., Zorzi, M., de Schotten, M.T., Corbetta, M., 2020. Post-stroke deficit prediction from lesion and indirect structural and functional disconnection. Brain 143, 2173. https://doi.org/10.1093/BRAIN/AWAA156.

Schott, J.M., Crutch, S.J., 2019. Posterior Cortical Atrophy. Contin. Lifelong Learn. Neurol. https://doi.org/10.1212/CON.0000000000000696.

Serra, L., Gabrielli, G.B., Tuzzi, E., Spanò, B., Giulietti, G., Failoni, V., Marra, C., Caltagirone, C., Koch, G., Cercignani, M., Bozzali, M., 2017. Damage to the frontal aslant tract accounts for visuo-constructive deficits in Alzheimer's Disease. J. Alzheimer's Dis. 60, 1015–1024. https://doi.org/10.3233/JAD-170638.

Siless, V., Chang, K., Fischl, B., Yendiki, A., 2017. AnatomiCuts: hierarchical clustering of tractography streamlines based on anatomical similarity. Neuroimage 166, 32. https://doi.org/10.1016/J.NEUROIMAGE.2017.10.058.

Singh, N.A., Goodrich, A.W., Graff-Radford, J., Machulda, M.M., Sintini, I., Carlos, A.F., Robinson, C.G., Reid, R.I., Lowe, V.J., Jack, C.R., Petersen, R.C., Boeve, B.F., Josephs, K.A., Kantarci, K., Whitwell, J.L., 2024. Altered structural and functional connectivity in Posterior Cortical Atrophy and dementia with lewy bodies. Neuroimage 290, 120564. https://doi.org/10.1016/J.NEUROIMAGE.2024.120564.

Smith, S.M., Nichols, T.E., 2009. Threshold-free cluster enhancement: Addressing problems of smoothing, threshold dependence and localisation in cluster inference. Neuroimage 44, 83–98. https://doi.org/10.1016/J.NEUROIMAGE.2008.03.061.

Smits, A.R., van Zandvoort, M.J.E., Ramsey, N.F., de Haan, E.H.F., Raemaekers, M., 2023. Reliability and validity of DTI-based indirect disconnection measures. Neuroimage Clin. 39, 103470. https://doi.org/10.1016/J.NICL.2023.103470.

Snowden, J.S., Stopford, C.L., Julien, C.L., Thompson, J.C., Davidson, Y., Gibbons, L., Pritchard, A., Lendon, C.L., Richardson, A.M., Varma, A., Neary, D., Mann, D.M.A., 2007. Cognitive phenotypes in Alzheimer's disease and genetic risk. Cortex 43, 835–845. https://doi.org/10.1016/S0010-9452(08)70683-X.

Tang-Wai, D.F., Graff-Radford, N.R., Boeve, B.F., Dickson, D.W., Parisi, J.E., Crook, R., Caselli, R.J., Knopman, D.S., Petersen, R.C., 2004. Clinical, genetic, and neuropathologic characteristics of Posterior Cortical Atrophy. Neurology 63, 1168–1174. https://doi.org/10.1212/01.WNL.0000140289.18472.15.

Van Essen, D.C., Smith, S.M., Barch, D.M., Behrens, T.E.J., Yacoub, E., Ugurbil, K., 2013. The WU-minn human connectome project: an overview. Neuroimage 80, 62–79. https://doi.org/10.1016/j.neuroimage.2013.05.041.

Velioglu, H.A., Ayyildiz, B., Ayyildiz, S., Sutcubasi, B., Hanoglu, L., Bayraktaroglu, Z., Yulug, B., 2023. A structural and resting-state functional connectivity investigation of the pulvinar in elderly individuals and Alzheimer's disease patients. Alzheimer'S Dement. 19, 2774–2789. https://doi.org/10.1002/ALZ.12850.

Wang, J., Tao, W., Chu, M., Jiang, D., Liu, L., Cui, Y., Liu, Y., Wang, Y., Han, Y., Yang, C., Wu, L., 2024. Alterations of the pulvinar in Posterior Cortical Atrophy: a multimodal MRI study. Cortex 181, 311–321. https://doi.org/10.1016/j.cortex.2024.08.007.

Wells, G.A., Wells, G., Shea, B., Shea, B., O'Connell, D., Peterson, J., Welch, Losos, M., Tugwell, P., Ga, S.W., Zello, G.A., Petersen, J.A., 2014. The Newcastle-Ottawa Scale (NOS) for Assessing the Quality of Nonrandomised Studies in Meta-Analyses.

Wen, Q., Mustafi, S.M., Li, J., Risacher, S.L., Tallman, E., Brown, S.A., West, J.D., Harezlak, J., Farlow, M.R., Unverzagt, F.W., Gao, S., Apostolova, L.G., Saykin, A.J., Wu, Y.C., 2019. White matter alterations in early-stage Alzheimer's disease: a tract-specific study. Alzheimer'S Dement. Diagn. Assess. Dis. Monit. 11, 576–587. https://doi.org/10.1016/J.DADM.2019.06.003.

Whitwell, J.L., Jack, C.R., Kantarci, K., Weigand, S.D., Boeve, B.F., Knopman, D.S., Drubach, D.A., Tang-Wai, D.F., Petersen, R.C., Josephs, K.A., 2007. Imaging correlates of Posterior Cortical Atrophy. Neurobiol. Aging 28, 1051–1061. https://doi.org/10.1016/j.neurobiolaging.2006.05.026.

Whitwell, J.L., Graff-Radford, J., Singh, T.D., Drubach, D.A., Senjem, M.L., Spychalla, A. J., Tosakulwong, N., Lowe, V.J., Josephs, K.A., 2017. 18F-FDG PET in Posterior Cortical Atrophy and dementia with lewy bodies. J. Nucl. Med. 58, 632–638. https://doi.org/10.2967/jnumed.116.179903.

Yang, C., Gao, X., Liu, N., Sun, H., Gong, Q., Yao, L., Lui, S., 2023. Convergent and distinct neural structural and functional patterns of mild cognitive impairment: a multimodal meta-analysis. Cereb. Cortex 33, 8876–8889. https://doi.org/10.1093/CERCOR/BHAD167.

Yeh, F.C., 2020. Shape analysis of the human association pathways. Neuroimage 223, 117329. https://doi.org/10.1016/J.NEUROIMAGE.2020.117329.

Yeh, F.C., 2022. Population-based tract-to-region connectome of the human brain and its hierarchical topology. Nat. Commun. 2022 13, 1–13. https://doi.org/10.1038/s41467-022-32595-4.

Yeh, F.C., Tseng, W.Y.I., 2011. NTU-90: a high angular resolution brain atlas constructed by q-space diffeomorphic reconstruction. Neuroimage 58, 91–99. https://doi.org/10.1016/j.neuroimage.2011.06.021.

Yeh, F.C., Wedeen, V.J., Tseng, W.Y.I., 2010. Generalized q-sampling imaging. IEEE Trans. Med. Imaging 29, 1626–1635. https://doi.org/10.1109/TMI.2010.2045126.

Yeh, F.C., Panesar, S., Fernandes, D., Meola, A., Yoshino, M., Fernandez-Miranda, J.C., Vettel, J.M., Verstynen, T., 2018. Population-averaged atlas of the macroscale human structural connectome and its network topology. Neuroimage 178, 57–68. https://doi.org/10.1016/J.NEUROIMAGE.2018.05.027.

Yeh, F.C., Panesar, S., Barrios, J., Fernandes, D., Abhinav, K., Meola, A., Fernandez-Miranda, J.C., 2019. Automatic removal of false connections in diffusion MRI tractography using topology-informed pruning (TIP). Neurotherapeutics 16, 52–58. https://doi.org/10.1007/S13311-018-0663-Y.